In: Kruhl JH (Ed.)
Fractals and Dynamic Systems in Geoscience.
Springer, Berlin, 1994.

Application of the Grassberger-Procaccia Algorithm to the $\delta^{18}O$ Record from ODP Site 659: Selected Methodical Aspects

Manfred Mudelsee & Karl Stattegger
Graduiertenkolleg "Dynamik globaler Kreisläufe im System Erde",
Geologisch-Paläontologisches Institut und Museum, Universität Kiel,
Olshausenstr. 40, D-24118 Kiel, Germany

Abstract. The Grassberger-Procaccia algorithm, which allows one to estimate the correlation dimension of a chaotic system, was investigated on oxygen isotope data from the deep-sea sediment core ODP Site 659 from the eastern North Atlantic. These data provide uniform coverage of the last 5.2 Ma and show an average spacing of 4.5 ka (1170 points). They are assumed to reflect global ice volume as a proxy for global climate.

This paper focusses on methodical aspects. One important point consists in the use of nonlinear fits instead of linear fits after a logarithm transformation. The latter overestimates the correlation dimension. An advantage is that the comparable large amount of original data allowed the number of (equidistant) working-data points (generated by linear interpolation) to be held equal to the number of original data points in order to strive for small statistical dependences between the working-points.

The Pliocene and Pleistocene climatic signatures can clearly be distinguished in the reconstructed space of climatic states.

The behavior of the estimated correlation dimension on the embedding dimension does not indicate the existence of a low-dimensional attractor. The behavior on a variable time lag does not indicate a definite lower boundary for the time lag above 4.5 ka. The behavior on the fit region shows a strong dependence on the upper boundary for the region, whereas the dependence on the lower boundary is weak.

Introduction

Correlation Dimension and the Grassberger-Procaccia Algorithm

The correlation dimension (D) has become an important descriptive parameter of chaotic systems; it is sensitive to the dynamical processes of coverage of the attractor shown by this system, in contrast to the fractal dimension which describes the geometry of the attractor. (The latter has an upper boundary in D.) The correlation dimension can be of importance for constructing models of such systems, e.g., a low value of D would indicate the possibility of describing the system by a low number of deterministic equations. Advantageously, the correlation dimension can be calculated from a single time series of a system by

reconstructing the system's trajectory in an "embedding space" (Packard et al. 1980, Takens 1981, Ruelle 1981, Grassberger & Procaccia 1983). To construct the embedding space, a time lag is introduced by which the time series is successively shifted. The dimension of the trajectory, and thus the correlation dimension, can be calculated using the algorithm of Grassberger & Procaccia (1983) (in addition to different algorithms). Hereafter, the whole procedure is called the GP-method. It is outlined briefly below.

Given an equidistant time series,

$$X(1), X(2), ..., X(N),$$

with a certain spacing and a certain number N of data points, the embedding space is constructed by means of Y vectors:

$$\begin{aligned} Y(1) &= [X(1), X(1+L), X(1+2L), ..., X(1+(M-1)L)], \\ Y(2) &= [X(2), X(2+L), X(2+2L), ..., X(2+(M-1)L)], \\ &\vdots \quad \vdots \quad \vdots \quad \vdots \quad \vdots \\ Y(p) &= [X(p), X(p+L), X(p+2L), ..., X(p+(M-1)L)]; \end{aligned} \tag{1}$$

where L denotes a time lag (measured in units of the data spacing) and M is the embedding dimension. Notice that the number p of vectors is given by N-(M-1)L. Each vector Y corresponds to a point in the embedding space and defines a certain state of the system which is described by the time series (ODP 659 data, Fig. 4).

The Grassberger-Procaccia algorithm introduces the correlation integral, also called correlation function, C(r),

$$C(r) = \text{factor} \times \text{sum of distances } |Y(i)-Y(j)| \text{ smaller than } r.$$

(The symbol r denotes the distance between points in the embedding space and should not be confused with the correlation coefficient.) For our purposes, the (normation) factor is set to 1/2 accounting for the symmetry in i, j of distances.

Grassberger & Procaccia (1983) showed that for "large" M and "small" r the following relation holds true provided an attractor exists:

$$C(r) \propto r^{D} \tag{2}$$

In practice, the correlation dimension D is determined by setting M=1,2,3, ... and estimating a power-law relation between r and C(r). This is usually carried out by means of linear least-squares regression on the logarithmically transformed data. If the value of the estimated exponent of the power-law relation saturates with growing *M*, this saturation value is taken as the best estimate of D. On the contrary, a white noise process, for which no attractor exists, would not produce a saturation behavior of the exponent (Fig. 1). Strictly speaking, one should use the term "correlation dimension" only when saturation occurs. In the text, however, we have adopted it synonymously to the exponent of the power-law relation.

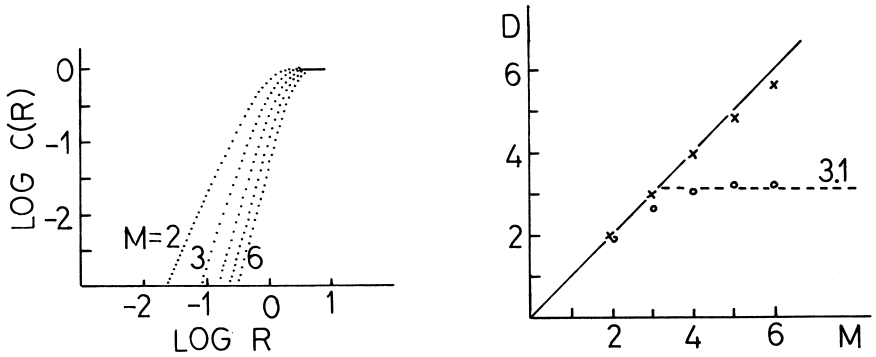

Fig. 1. Redrawn after Nicolis & Nicolis (1984), with modified notation. Left panel: Correlation functions in double-log plot for different choices of M (note that the normation factor (section "Correlation dimension...") is different to that used in this chapter); the linear range gives the slope, D. Right panel: D versus M; the saturation-like behavior for the climate data (circles) led to the conclusion of Nicolis & Nicolis (1984) that an attractor exists with $D \approx 3.1$ for the long-term climatic system. The white noise process (x) does not show a saturation behavior.

The Grassberger-Procaccia (GP) Method Applied to Experimental Data

Describing complex natural systems is often done by starting with basic equations given by the natural laws considered as necessary for the description of the system. From these a set of, usually coupled, differential equations is derived which describe the behavior of the system. One example is the Lorenz model in meteorology (Lorenz 1963). From the differential equations a, theoretically, unlimited number of noise-free data points can be derived. Those "theoretical" systems allow efficiently converging calculations of the correlation dimension with the GP-method (Ben-Mizrachi et al. 1984).

However, when the governing equations of a natural system are generally unknown, calculation of the correlation dimension with the GP-method must be done using experimental data which are generally limited in number and influenced by noise. Therefore, some points of critique have been raised concerning the GP-method applied to experimental data:

(a) *Number of data points*, N. Figure 5a, from ODP 659 data, shows the saturation behavior of C(r) for large r, where the power-law (Eq. 2) does not hold true anymore. Regression comprising this region of r would yield a dimension, D, that is too low. The fit region, therefore, has an upper boundary, r_U. It has been shown that for too high choices of M (with N fixed) the value of r_U diminishes and, hence, the possibility to determine the exponent also diminishes. The maximum meaningful value of M grows with N; however, a uniformly accepted formula N(M) does not exist yet. For example, if $N \approx 1000$, a maximum value of $M \approx 4$ can be derived following

Theiler (1986), a maximum value of $D \approx 5.5$ can be derived from the slightly corrected formula of Eckmann & Ruelle (1992).

(b) *Time lag*, L. In order to cover an attractor without any preference for a certain region of it, the vectors Y(i) should be statistically independent of each other. This can be achieved by using a high value of L. Alternatively, as suggested by Theiler (1986), the summation in the correlation integral about the distances $|Y(i)-Y(j)|$ could involve the condition that $|i-j|$ should be high enough to exclude statistically dependent pairs Y(i), Y(j). On the other hand very high values of L lead to the loss of information on finer time scales. A generally accepted relation is (e.g. Maasch 1989):

$$L \approx \text{correlation time of the time series}$$

(for the determination of the correlation time, see below). In addition, we stress that another source of statistical dependence between the vectors Y(i) is introduced by the initial interpolation of the data points in order to get equidistant points. This dependence increases if more working-points are generated than data points existed originally.

(c) *Experimental noise*. It is comprehensible that a fit region below a certain value, r_L, does not make sense because a finite distance between two vectors, Y(i) and Y(j), is already given by the error of the experimental data. It has been shown (Ben-Mizrachi et al. 1984) that r_L should be in the order of this experimental noise amplitude.

More details about the role of N, L and the "scaling region" (that is the interval $[r_L, r_U]$) are given in: Lochner et al. (1989), Nerenberg & Essex (1990).

(d) *Colored noise*. A basic point of critique has been raised by Osborne and Provenzale (1989) who showed that some stochastic processes (colored noise) also exhibit a finite correlation dimension. Onto that, we emphasize studying the following topics more intensively: the multiplicative interaction between variables describing complex natural systems, the impact of this interaction on the shape of the distribution function, i.e. the color of the noise, of these variables and the significance of the lognormal distribution (Aitchison & Brown 1957) for the description of such systems.

Since 1983, the GP-method has been applied to experimental data from natural systems. The data cover different temporal and spatial scales. Nicolis & Nicolis (1984) claimed the existence of a definite, low-dimensional attractor ($D = 3.1$) for the long-term global climate system (Fig. 1). They used the $\delta^{18}O$ record of the deep-sea sediment core V28-238 which covers the last 800 ka and consists of ≈200 data points. This result was subsequently criticized by Grassberger (1986) who warned that "spuriously small dimension estimates can be obtained from using too few, too finely sampled and too highly smoothed data". Maasch (1989) investigated 14 Pleistocene $\delta^{18}O$ records and concluded that an attractor exists with D in the range 4-6.

In this work we have concentrated on selected methodical aspects of the application of the GP-method to experimental data: From the above critique we have investigated point (b) and, less extensively, points (a) and (c). As data source we have chosen a $\delta^{18}O$ record covering a longer time interval and containing more data points than the records used in the publications mentioned above. This experimental time series contains the maximum of data currently available in paleoclimatology, but still is relatively „short" in comparison to "theortical" systems.

Additionally, of significant importance, we show that the commonly practised way of fitting the power-law behavior of C(r) (Eq. 2) in order to estimate the correlation dimension systematically overestimates the latter. Instead of using double-log plots and linear fits we use nonlinear fits.

Global Long-Term Climatic Variations Recorded from Deep-Sea Core ODP Site 659

Time Series

Data source is the deep-sea sediment core ODP Site 659, recovered during the Ocean Drilling Program, from the eastern North Atlantic (18°04.63'N, 21°01.57'W) at a water depth of 3070 m (Sarnthein & Tiedemann 1989). Specimens of the benthic foraminifer *Cibicidoides wuellerstorfi* ($CaCO_3$ shell), size fraction 250-315µm, were taken to measure by means of a mass spectrometer the oxygen isotope ratios relative to a standard (PDB):

$$\delta^{18}O\ [‰] = [(^{18}O/^{16}O)_{sample} - (^{18}O/^{16}O)_{PDB}]/(^{18}O/^{16}O)_{PDB} \times 1000$$

The average, absolute uncertainty of the $\delta^{18}O$ values is 0.07 ‰.

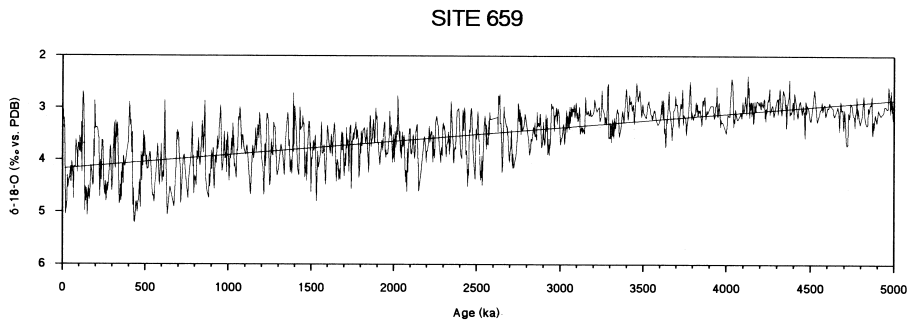

Fig. 2. The time series: oxygen isotope record for the ODP Site 659, 0-5000 ka (Tiedemann et al., in press), linear trend; for further explanation see the text.

Autocorrelation Function

These data are assumed to reflect the global ice volume as a proxy for global climate (low values: "warm"/"less land-ice", high values: "cold"/"much land-ice"). The time scale (Figure 2, Tiedemann et al., in press) was achieved by determining magnetic and biostratigraphic events in the core and then tuning the time scale between these events by means of the calculated temporal behavior of the parameters of the Earth's orbit (which act as "pacemakers" for the global long-term climate, see, e.g., Hays et al. 1976, Imbrie et al. 1984). The core shows no hiatuses, the number of original data points, N, is 1170, the maximum age is 5268 ka, the average spacing is 4.5 ka. The linear trend (≈- 0.266 ‰ /ka) is also shown in Fig. 2.
Subtracting the linear trend permitted calculation of the autocorrelation function of the time series (Figure 3); its first zero crossing, which is generally recommended as an estimate of the correlation time (e.g., Maasch 1989), is 23.4 ka. This value corresponds closely to the Milankovitch precession period of 23 ka (Berger & Loutre 1991).

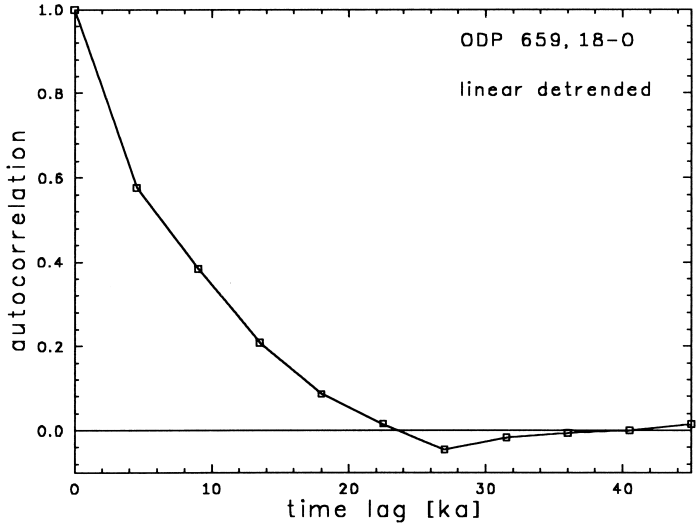

Fig. 3. Autocorrelation function of the linear detrended time series (Fig. 2); the first zero crossing occurs at the time lag 23.4 ka.

Embedding Space

In order to obtain equidistant working-points, the original data (not detrended) were interpolated by a linear interpolation. This seemed to be acceptable since it reduced the variance, and, hence, the stored information, of the original data by

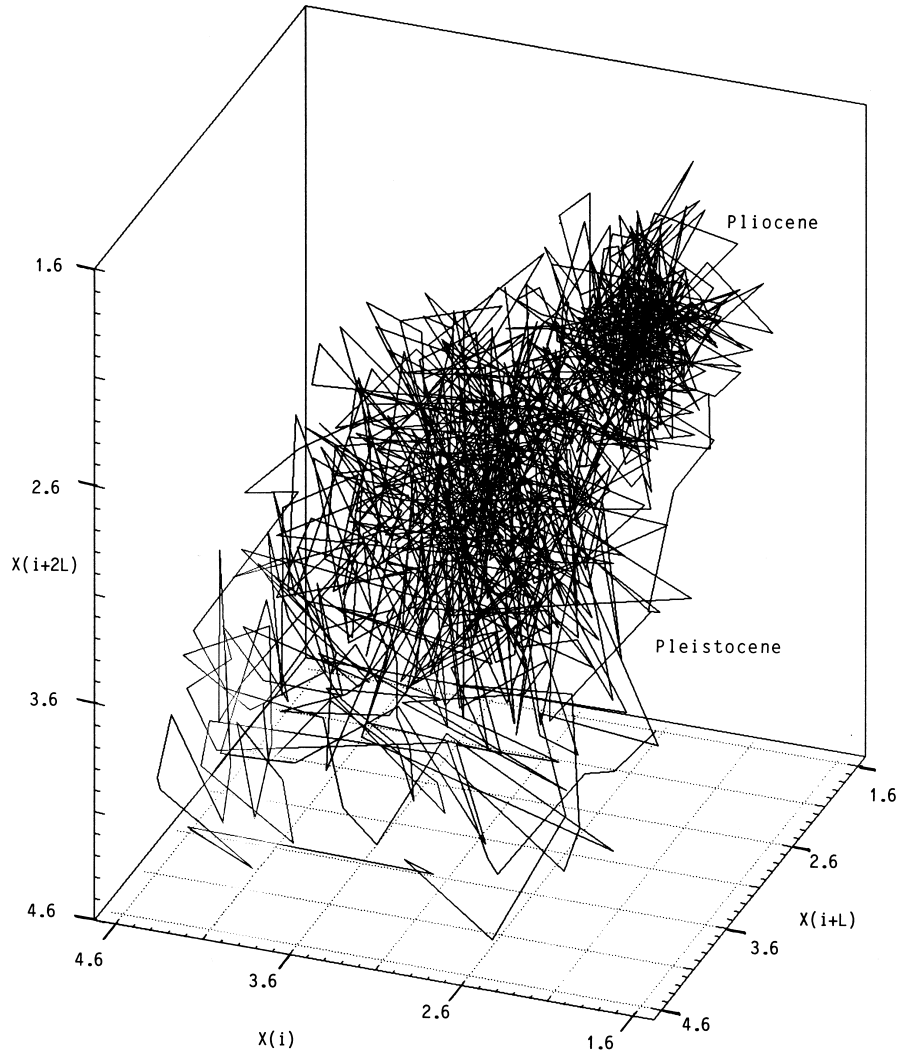

Fig. 4. Embedding space, constructed with M=3, L=3 for the time series. Units are ‰ vs. PDB. A point Y(i) is given by [X(i), X(i+L), X(i+2L)] (Eq. 1) and defines the state of the climatic system at a certain time. The connection of consecutive points ("trajectory") in the embedding space reflects the temporal behavior of the system. The correlation dimension describes such sometimes strange-looking objects ("strange attractors") not only geometrically but as well notices the "density" of points in the embedding space.

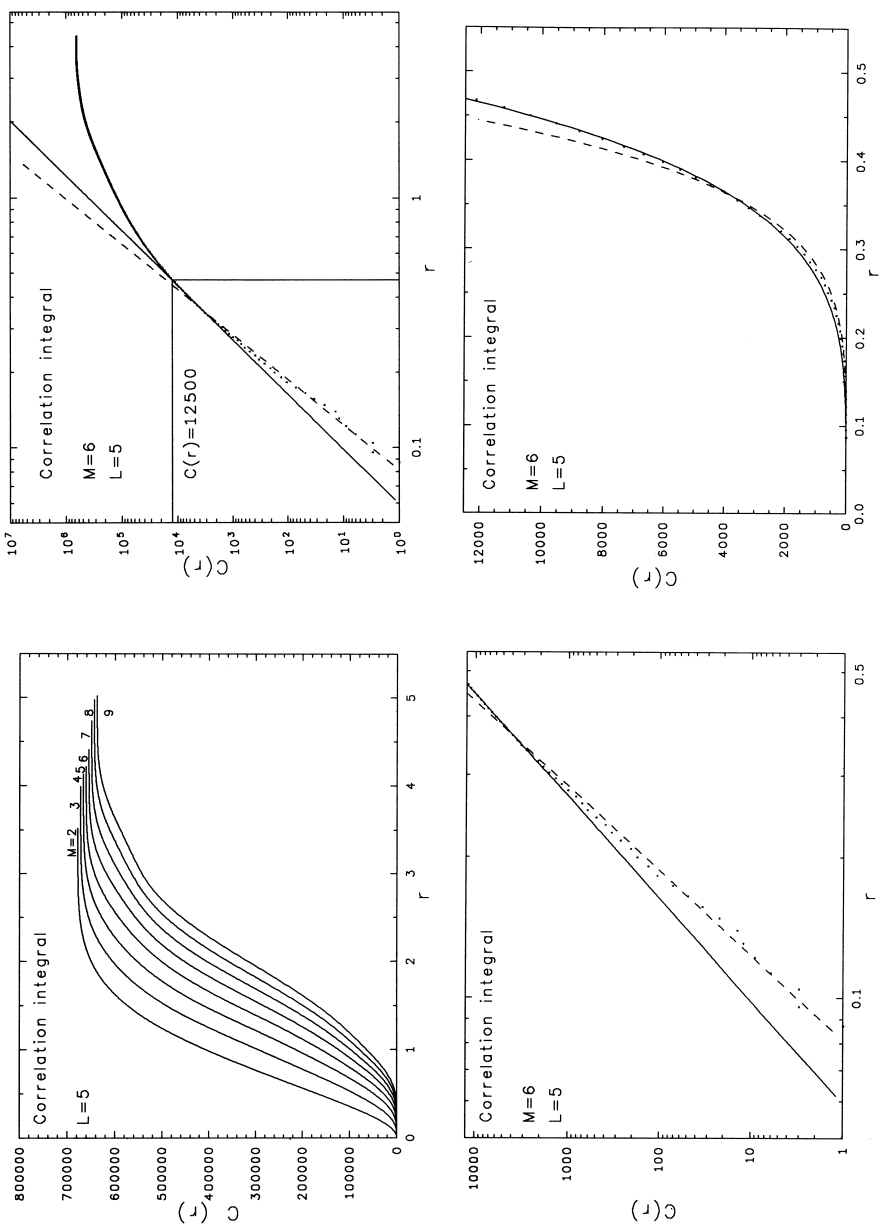

Fig. 5 b d
a c

only 4%. The number of working-points was held equal to the number of original data points in order to avoid the enhancement of the statistical dependence between the vectors Y(i) (above, section "The GP-Method...", point b). Figure 4 shows the system's trajectory in the embedding space for a certain choice of M and L. There appear to be *two* clouds of points, representing two climatic states ["Pliocene": older part of the time series (Fig. 2), showing lower oxygen isotope values and smaller oscillations; "Pleistocene": younger part of the time series, showing higher oxygen isotope values and larger oscillations]. One possibility would be to substract the linear trend from the time series, the other would be to investigate these distinct time intervals separately. First of all, however, we show the results using the entire range of the original data.

Correlation Integral

The correlation integral, C(r), was determined for M = 2,...,9 and L = 1,...,9 (Figure 5a). L is measured in units of the spacing (4.5 ka) of the equidistant points.

Double-log plots and linear fits: overestimating the correlation dimension

Figure 5b shows the correlation function for a certain choice of M and L in a double-log plot. The latter is the basis for the commonly practised way of regressing the original model

$$C(r) \propto r^{D}$$

Fig. 5a-d. a Correlation integral, calculated with L=5, M=2,...,9 in linear plot for the entire scale of distances, r. Note the power-law-like growth of C(r) for small r, the saturation behavior for large r (which corresponds to the limited extension of objects like those shown in Fig. 4), and the saturation value of p(p-1)/2 (p is the number of vectors in the embedding space, see section "Correlation Dimension..."). Increasing values of M generally yield larger distances and a lower saturation value. **b** Correlation integral (dots), calculated with L=5, M=6 in double-log plot. [Because of the unequally spaced values of log (r) the dots representing higher values of r are not resolved and appear as a thick line. In Fig. 5d, using a linear plot, the r-values are equally spaced.] The scaling region corresponds to C(r) < 12500 and is marked. The best linear fit (dashed) using this scaling region yields the slope, i.e. D = 5.53±0.05; the best power-law fit (solid; see Eq. 2), using the same scaling region and the linear plot, yields D = 4.57±0.03. **c** Same as in Figure 5b, focussing on the scaling region. **d** Same as in Figure 5c, but using linear scales for r and C(r). The superiority of the nonlinear power-law fit over the linear fit after the logarithm transformation is demonstrated. The sum of squared residuals of 3.70×10^{5} from the nonlinear fit in comparison with 3.83×10^{7} from the linear fit after the logarithm transformation underlines this observation. The superiority was noticed for all other values of L and M.

and consists of taking the logarithms and then fitting a straight line to the transformed data:

$$\log[C(r)] = \text{const.} + D \times \log[r].$$

Thus, the slope estimates the correlation dimension. The alternative regression of the model consists in nonlinear (power-law) fits to the original model. This method demands numerical calculations and is generally neglected in favor of the double-log plots.

Also plotted in Fig. 5b is the best linear fit (dashed) using the following scaling region:
r_L = minimum value of r, r_U corresponds to C(r) < 12500. This fit yields a slope, i.e. D = 5.53±0.05 (1 sigma) and a sum of squared residuals of 3.83×10^7. The sum of squared residuals measures the deviation of the fit function from the data points. The nonlinear regression (solid), using the same scaling region yields D = 4.57 ± 0.03 and a sum of squared residuals of 3.70×10^5. Thus, *the same data points are more precisely described by the nonlinear regression than by the linear regression after logarithm transformation*. Figures 5c and 5d focus on thescaling region, whereby Fig. 5d demonstrates visually the superiority of the nonlinear regression for the "true" relationship, $C(r) \propto r^D$. The statement that the loss of the equal spacing between the r-values (when they are logarithmically transformed) would produce this difference is refuted: The same difference results if in the double-log plot the spacing between the r-values is equidistant (compare Fig. 5b). The fact that the linear fit after a log-log transformation systematically overestimates the correlation dimension is explained by the following two points: (1) When assuming the original power-law relationship for true, the log-log transformation produces a violation of the Gauss-Markov conditions for least-squares regression, such that a biased estimation results (Sen & Srivastava 1990, page 35; see also Schulz et al. 1994). (2) The *over*estimation results from the monotonic growth of the power-law function for positive exponents. Additionally, the systematic deviation from the power-law, i.e. the saturation behavior, growing with r, may also contribute to this effect. We, therefore, choose the nonlinear regression method in order to estimate D. The problem of the inadequacy of linear transformations for regression purposes (e.g. for a power-law function) has been demonstrated, e.g. by Rützel (1976).

Scaling Region

Concerning the scaling region: as the experimental noise is considerably weak, the results from taking r_L in the magnitude of the noise or instead taking r_L = minimum value of r differ only very little from each other; the important value is r_U. Here we decided to determine r_U corresponding to several permitted maximum values of C(r), i.e.:

C(r) < 50000 (or 25000, 12500, 6250, 3125.) We know that this is only a first attempt. An indepth investigation of the problem of the proper choice of the scaling region must choose whether to define the scaling region via boundaries in C(r) (as we have done) or boundaries in r, or to measure the quality of the regression and using that interval which yields the best fit. Also the spacing for the distances, r, is still arbitrary and should be investigated.

Results

The following dependences of the estimated correlation dimension on the parameters time lag, scaling region, and embedding dimension resulted:

(i) *The dependence of the correlation dimension*, D, *on the time lag*, L, (Fig. 6) shows that the value of D is not strongly influenced by L above 1 (4.5 ka). Therefore, the above stated recommendation, to choose L to be in the order of the correlation time (23.4 ka), does not seem to be a necessary condition for the determination of D.

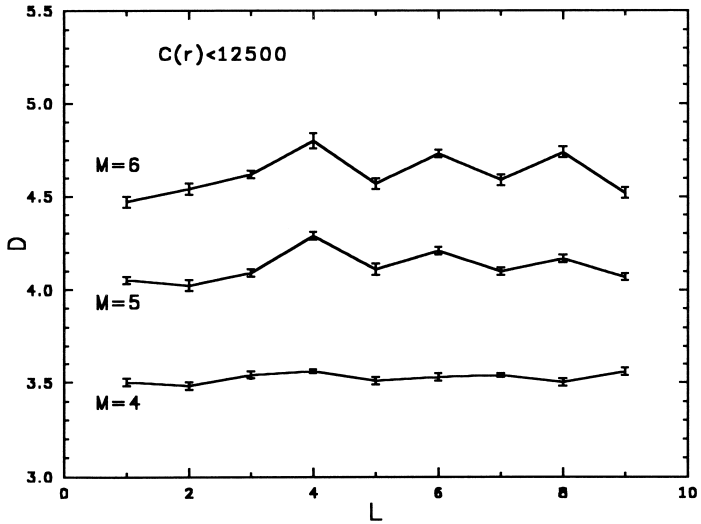

Fig. 6. Dependence of the estimated correlation dimension, D, on the time lag, L, for three different values of M. The values of D result from nonlinear regression and r_U corresponds to C(r) < 12500. L is measured in units of the spacing (4.5 ka) of the time series. The error bars represent the average standard deviation of the estimated correlation dimension.

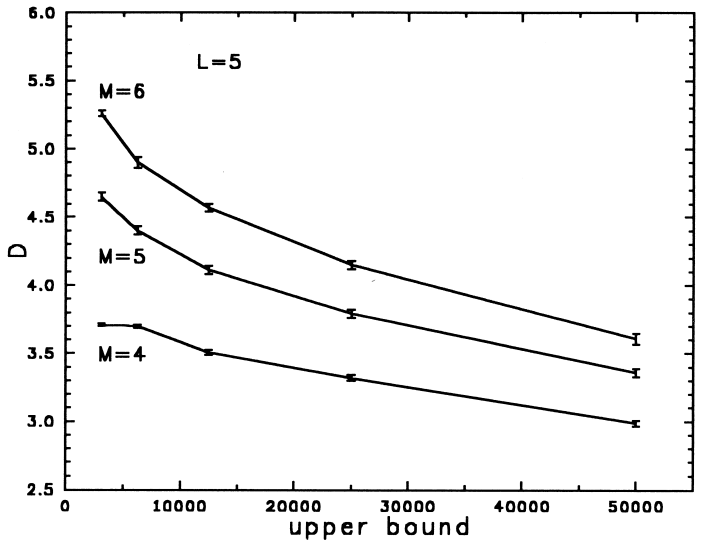

Fig. 7. Dependence of the estimated correlation dimension, D, on the fit range (scaling region) for three different values of M. The values of D result from nonlinear regression and the time lag L=5. The fit range [r_L, r_U] was: r_L = minimum value of r; the upper boundary, r_U, corresponds to C(r) < 50000, resp., 25000, 12500, 6250, 3125 (x-axis).

(ii) *The dependence on the scaling region* (Fig. 7) underlines the strong influence of the upper boundary, r_U. However, our method of handling the problem of the proper choice of the scaling region is not sufficient to give a detailed recommendation.

(iii) *The dependence of the correlation dimension*, D, *on the embedding dimension*, M, (Fig. 8), displays no saturation behavior. Hence, no low-dimensional attractor exists for the investigated climate system. This statement holds true also when the uncertainties concerning the proper choice of the time lag, L, and the upper boundary of the scaling region, r_U, are considered. As Figures 6 and 7 show, for a variety of values of L and r_U the correlation dimension, D, increases when M is increased. When following the restriction M < 5, respectively D < 5.5, from above (section "The GP-method...", a) due to the limited number of data points, the statement changes to: there is no attractor with D < 4 (fig. 8), respectively D < 5.5. This high dimension of the attractor compounds further the problem of „short" time series.

(iv) In addition, all calculations were performed on the *linear detrended* data points (compare Fig. 3) yielding the *same* results.

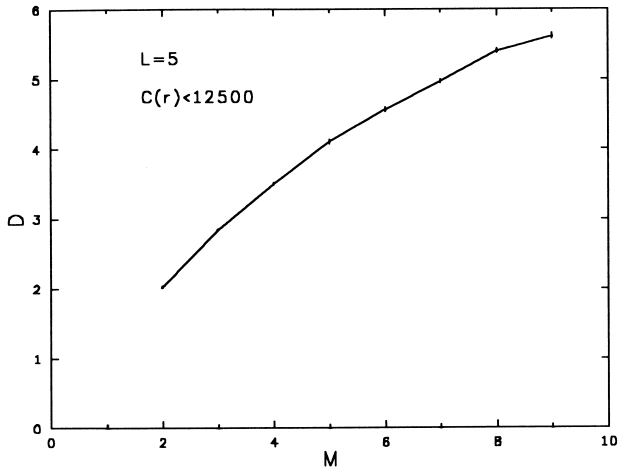

Fig. 8. Dependence of the estimated correlation dimension, D, on the embedding dimension, M. The values of D result from nonlinear regression. The time lag, L, is 5, and r_U corresponds to C(r) < 12500.

Conclusions

The Grassberger-Procaccia method to estimate the correlation dimension from a time series was applied to paleoceanographic data which reflect the global climatic variations over the last five million years.

It can be shown that the conventionally used double-log plots and linear fits systematically overestimate the correlation dimension. Therefore, nonlinear fits need to be calculated.

The value of the time lag, L, while greater than 4.5 ka, does not have a strong influence on the estimated dimension.

The choice of the upper boundary of the scaling region, r_U, however, does have a strong influence on the estimated dimension. This effect will be studied in detail in the future.

Based on the present state of the GP-method we conclude: the long-term climatic system described by our deep-sea sediment core does not show a low-dimensional attractor.

Finally, considering the points of critique from above, we suspect that by the means of the GP-method, at the present state of knowledge, only the rejection of low-dimensional attractors in natural systems may be possible.

Our future research will include the investigation of (i) distinct time intervals, e.g. the Pliocene ("warm") and the Pleistocene ("cold" / "oscillating"); (ii) additional high-resolution paleoclimatic data records; and (iii) synthetic time series for comparison purposes.

Acknowledgements. We gratefully acknowledge R. Tiedemann for providing the data material, a diagram and information about ODP Site 659. K. Herterich and K.A. Maasch made valuable review comments. P. Dingle refined the English of the manuscript. The Graduiertenkolleg "Dynamik globaler Kreisläufe im System Erde" is sponsored by the Deutsche Forschungsgemeinschaft.

References

Aitchison J, Brown JAC (1957) The lognormal distribution. Cambridge University Press, Cambridge.

Ben-Mizrachi A, Procaccia I, Grassberger P (1984) Characterization of experimental (noisy) strange attractors. Phys Rev A 29: 975-977.

Berger A, Loutre MF (1991) Insolation values for the climate of the last 10 million years. Quat Sci Rev 10: 297-317.

Eckmann, J-P, Ruelle D (1992) Fundamental limitations for estimating dimensions and Lyapunov exponents in dynamical systems. Physica D 56: 185-187.

Grassberger P (1986) Do climatic attractors exist? Nature 323: 609-612.

Grassberger P, Procaccia I (1983) Characterization of strange attractors. Phys Rev Lett 50: 346-349.

Hays JD, Imbrie J, Shackleton NJ (1976) Variations in the Earth's orbit: pacemaker of the ice ages. Science 194: 1121-1132.

Imbrie J, Hays JD, Martinson DG, McIntyre A, Mix AC, Morley JJ, Pisias NG, Prell WL, Shackleton NJ (1984) The orbital theory of Pleistocene climate: support from a revised chronology of the marine $\delta^{18}O$ record. In: Berger A, Imbrie J, Hays JD, Kukla G, Saltzman B (eds) Milankovitch and Climate, Part I. Reidel, Dordrecht, pp 269-305.

Lochner JC, Swank JH, Szymkowiak AE (1989) A search for a dynamical attractor in Cygnus X-1. Astrophys J 337: 823-831.

Lorenz EN (1963) Deterministic nonperiodic flow. J Atmos Sci 20: 130-141.

Maasch KA (1989) Calculating climate attractor dimension from $\delta^{18}O$ records by the Grassberger-Procaccia algorithm. Clim Dynam 4: 45-55.

Nerenberg MAH, Essex C (1990) Correlation dimension and systematic geometric effects. Phys Rev A 42: 7065-7074.

Nicolis C, Nicolis G (1984) Is there a climatic attractor? Nature 311: 529-532.

Osborne AR, Provenzale A (1989) Finite correlation dimension for stochastic systems with power-law spectra. Physica D 35: 357-381.

Packard NH, Crutchfield JP, Farmer JD, Shaw RS (1980) Geometry from a time series. Phys Rev Lett 45: 712-716.

Ruelle D (1981) Chemical kinetics and differentiable systems. In: Pacault A, Vidal C (eds) Nonlinear phenomena in chemical dynamics. Springer, Berlin Heidelberg New York, pp 30-37.

Rützel E (1976) Zur Ausgleichsrechnung: Die Unbrauchbarkeit von Linearisierungsmethoden beim Anpassen von Potenz- und Exponentialfunktionen. Archiv für Psychologie 128: 316-322.

Sarnthein M, Tiedemann R (1989) Toward a high-resolution stable isotope stratigraphy of the last 3.4 million years: sites 658 and 659 off Northwest Africa. In: Ruddiman W, Sarnthein M, et al. (eds). Ocean Drilling Program, College Station, pp 167-185 (Proceedings of the Ocean Drilling Program, scientific results, vol 108).

Schulz M, Mudelsee M, Wolf-Welling TCW (1994) Fractal Analyses of Pleistocene Marine Oxygen Isotope Records. in: Kruhl JH (ed) Fractals and Dynamic Systems in Geoscience. Springer, Berlin Heidelberg New York, pp 377-387 (this volume).

Sen A, Srivastava M (1990) Regression analysis. Springer, Berlin Heidelberg New York.

Takens F (1981) Detecting strange attractors in turbulence. In: Rand DA, Young L-S (eds) Dynamical systems and turbulence. Springer, Berlin Heidelberg New York, pp 366-381 (Lecture notes in mathematics, vol 898).

Theiler J (1986) Spurious dimension from correlation algorithms applied to limited time-series data. Phys Rev A 34: 2427-2432.

Tiedemann R, Sarnthein M, Shackleton NJ (in press) Astronomic time scale for the Pliocene Atlantic $\delta^{18}O$ and dust flux records of ODP Site 659. Paleoceanography.